Gondwana Research 153 (2026) 60–72

Contents lists available at ScienceDirect

Gondwana Research

journal homepage: www.elsevier.com/locate/gr

Research Paper

Mantle eclogite evidence of subducted carbonate sediments in Earth's deep carbon cycle

Jing Sun [a,b,*], Ross N. Mitchell [c,d], Luc S. Doucet [e,f], Kouki Kitajima [g], Ranpeng Li [h], Jinglin Su [b], Qiqi Ou [i,j], Tanya Kalashnikova [k], Sergey I. Kostrovitsky [k]

[a] State Key laboratory of Petroleum Resources and Engineering, Beijing 102249, China
[b] College of Geosciences, China University of Petroleum, Beijing 102249, China
[c] State Key Laboratory of Lithospheric and Environmental Coevolution, Institute of Geology and Geophysics, Chinese Academic of Sciences 100029 Beijing, China
[d] School of Earth and Planetary Sciences, University of Chinese Academy of Sciences, Beijing 100049, China
[e] Department of Earth Research Group, TIGeR, School of Earth and Planetary Sciences, Curtin University, Perth, Western Australia 6102, Australia
[f] State Key Laboratory of Geological Processes and Mineral Resources, China University of Geosciences, Wuhan, Hubei 430074, China
[g] Department of Geoscience, University of Wisconsin-Madison, Madison, WI 53706, USA
[h] Department of Geological Sciences, University of Florida, 32611 Gainesville, Florida, USA
[i] Airborne Survey and Remote Sensing Center of Nuclear Industry, Shijiazhuang 050002, China
[j] High-resolution Earth Observation System Data Application Technical Support Center of Hebei Province, Shijiazhuang 050002, China
[k] Institute of Geochemistry, Siberian Branch of the Russian Academy of Sciences, 664033 Irkutsk, Russia

ARTICLE INFO

Keywords:
eclogite xenoliths
Mg isotopes
oxygen isotopes
mantle metasomatism
carbonate sediments

ABSTRACT

Mantle eclogite represents a rare and unique archive for understanding the dynamics and implications of subduction, but its origin is still debated especially for high-MgO eclogites. We report new chemical and Mg–O isotopic data on high-MgO mantle eclogites from the Obnazhennaya kimberlite, Siberia craton. Obnazhennaya high-MgO eclogites have lower bulk δ^{26}Mg isotopes (-1.47– -0.36‰) and mantle-like garnet δ^{18}O isotopes (+5.18–+6.39‰). A bulk mixing calculation among oceanic crust, carbonate sediment and kimberlite, and its effects on Mg isotopes and MgO content indicate that metasomatism can only increase the MgO content but not δ^{26}Mg, and more than 50% dolostone by mass is needed, under conditions with no kimberlitic melt metasomatism, to account for both high-MgO contents, which is unrealistically high for natural settings. The ternary mixing model on both O–Mg isotopic compositions and MgO–Mg isotopic compositions suggest that subducted oceanic crusts modified by mantle metasomatism (e.g., kimberlite-like melt) as well as carbonate sediments involvement collectively provides the best explanation for such a high magnesian origin. This model is also compatible with global mantle eclogite observations, where there is also a clear chemical composition distinction between high- and low-MgO eclogites globally. In light of our new results and global compilation, we propose that mantle eclogites represent a spectrum of metasomatized subducted oceanic crust with variable amounts of the involvement of carbonate sediments, the latter of which represents a novel ingredient in the recipe for making previously enigmatic high-MgO eclogite xenoliths in kimberlites.

1. Introduction

Earth's carbon cycle provides a first-order control on the concentration of oxygen and carbon dioxide in the atmosphere and oceans, which is essential in producing and maintaining a habitable planet (Berner, 2009; Giuliani et al., 2022). Carbon is stored in the oceanic lithospheric mantle, oceanic crust, and deep-sea sediments, particularly carbonates, and it is transported into the mantle by slab subduction (Muller et al., 2022) and partially returned to the surface by volcanic degassing (Dasgupta & Hirschmann, 2010; Wang et al., 2018; Zhang et al., 2022). However, the knowledge of the detailed behavior of deeply subducted carbonates is presently incomplete. Mantle eclogite xenoliths in kimberlites provide a rare and unique archive for potentially revealing the behavior of oceanic crust, sediments, and carbonate subducted deep into the mantle, and therefore the cryptic behavior of Earth's deep carbon cycle.

* Corresponding author.
E-mail address: sunjingvv@163.com (J. Sun).

https://doi.org/10.1016/j.gr.2025.11.015
Received 18 January 2025; Received in revised form 18 November 2025; Accepted 18 November 2025
Available online 13 December 2025

Eclogite xenoliths sometimes are divided into two groups based on their bulk MgO contents: low-MgO and high-MgO eclogite, where the threshold defining the high-MgO eclogite group ranges from 10–15% (Barth et al., 2001; Jacob, 2004). However, the origins of mantle eclogite are still debated (Aulbach et al., 2020a, 2020b; Wang et al., 2014, 2015; Huang et al., 2022), especially for high-MgO eclogite. Previous petrogenetic studies have suggested that high-MgO eclogite derive from a wide variety of potential origins: (i) high pressure mantle melt cumulates (e.g., Hills and Haggerty, 1989; Huang et al., 2022), (ii) reaction products due to element exchange between low-MgO eclogite and surrounding peridotite (e.g., Aulbach et al., 2002; Aulbach et al., 2007; Smart et al., 2009; Wang et al., 2015), and (iii) subducted oceanic crust (e.g., Barth et al., 2002; Tappe et al., 2011).

The Obnazhennaya ("Obn" for short) kimberlite pipe erupted at 151.8 ± 2.5 Ma (Sun et al., 2022) and lies within the Kuoika field, which occupies the northeastern-most portion of the Siberian craton. It contains low-MgO eclogite (MgO 13–16 wt.%) and high-MgO eclogite (MgO >16 wt.%) groups based on their estimated bulk MgO contents and distinct petrological characteristics. In this study, we report new Mg–O isotope data for a suite of eclogite xenoliths from the Obn kimberlite of the Siberia craton, as well as compile a comprehensive dataset of compositional and geochemical data for eclogite xenoliths globally. Our new Obn data shed light on the origin of eclogite xenoliths, and we attempt to show that the subduction of carbonate sediment plays a critical role in their compositions. Moreover, the model is then tested and confirmed with the global compilation, implying that mantle eclogites play an important role in Earth's deep carbon cycle.

2. Methods

2.1. Major elements analysis of minerals

Electron probe microanalysis (EPMA) of the major element compositions of Obn minerals were measured using the CAMECA SX-100 Electron Probe with 5 wavelength spectrometers at the University of California, Santa Barbara. A 15 keV accelerating voltage and a 10 nA beam current were used for the analysis. Multiple grains of the same minerals were analyzed from each sample, with a minimum of 5 analyses per mineral grain. A variety of natural and synthetic standards were used to calibrate the major components, some of which were also measured as unknowns to monitor data quality. The ZAF model (Armstrong, 1995) for the correction of matrix effects was applied. The 2σ analytical precision of most elements analyzed by EPMA is ~ 2%.

2.2. Trace elements analysis of minerals

Trace element compositions of Obn minerals were measured using laser ablation inductively coupled plasma mass spectrometry (LA-ICP-MS) at State Key Laboratory of Geological Processes and Mineral Resources, China University of Geoscience (GPMR-CUG). The operating conditions for LA-ICP-MS were the same as those described by Liu et al (2008). A 193 nm ArF excimer laser ablation system was used to laser samples with a spot size of 44 μm. An Agilent 7500a ICP-MS instrument was used to acquire ion-signal intensities. To correct the time-dependent drift of sensitivity and mass discrimination for the element analysis, NIST 610 was analyzed every 10 analyses. The element compositions were calibrated against multiple reference materials (BHVO-2G, BCR-2G and BIR-1G; Table A3; Liu et al., 2008). Offline selection and integration of background and analytical signals and time-drift correction and quantitative calibration were conducted using ICPMSDataCal (Liu et al., 2008). The detailed calibration strategy for accurate LA-ICP-MS analysis of trace elements in hydrous silicate minerals was reported in Chen et al (2014). The analytical precision of most elements analyzed by the LA-ICP-MS method is ~5–10%.

2.3. Oxygen isotope analysis of garnet

Oxygen isotope compositions of garnet were analyzed *in situ* using a CAMECA Secondary Ion Mass Spectrum (SIMS) IMS 1280 ion microprobe at the University of Wisconsin-Madison. Samples were lightly crushed and clean garnets (2–4 mm) were handpicked with a binocular microscope. Separated garnet grains were mounted within 7.5 mm of the center of an epoxy disk with the UWG-2 garnet standard at the center of the mount, and then polished to a flat, smooth surface. The $^{133}Cs^{+}$ primary ion beam (20 kV total accelerating voltage) was focused to a diameter of ~10 μm on the gold-coated sample surface. Secondary O^{-} ions were accelerated away from the sample by ~10 kV and the analysis site were centered under a uniform electric field generated by a normal-incidence electron gun for charging compensation. Due to the different compositions between garnet standard UWG-2 and the Obn garnets, a matrix effect is present. In order to account for the matrix effects,16 in-house garnet standards from 5 garnet end members (pyrope, almandine, spessartine, grossular, and andradite) were analyzed to calculate the working curve line and instrument bias relative to UWG-2 one day before running the unknowns. The Obn garnets were then plotted on the working curve line based on their compositions, and the bias of each unknown relative to UWG-2 was calculated. Details are provided in Page et al (2010) and Kitajima et al (2016), and we provide only a short summary here. Four points on UWG-2 were analyzed before and after every 20 unknown sample points (Table A4). The reference oxygen isotope (expressed as $\delta^{18}O$ relative to VSMOW) of UWG-2 standard is +5.8‰ (Valley et al. 1995). Point-to point precision for $\delta^{18}O$ was typically better than 0.34‰ (2 SD).

2.4. Mineral modal estimation

Modal abundances were obtained by counting the pixels of different minerals in thin section images. Garnet, clinopyroxene (cpx), orthopyroxene (opx), and melt veins have distinguishable features in the images of scanned thin sections, which can therefore be easily differentiated and marked. The percentages of minerals could be calculated by counting pixels of areas in the scanned images, using graphics editing software. Adobe Photoshop was used to mark different types of minerals by colors with different grey scales and Fiji ImageJ was used to calculate the pixels percentage of different gray scales. Kimberlitic melt veins are excluded in the calculation. We evaluated this method on a sample (7-303) from a previous study (Sun et al., 2020), whose modal abundance (47.5% garnet and 52.5% clinopyroxene) was calculated by point counting (47% garnet and 53% clinopyroxene) from the previous study. The result of pixels counting is 1% different from the point counting result. The 3D distribution and density of the minerals were not considered in this study, which may introduce some degree of modal uncertainty. In order to estimate the effect of modal uncertainty on the reconstructed bulk rock compositions, we calculated the major elements of the reconstructed bulk-rock composition of sample obn 7-359 with different mineral modal contents (Sup. Table A1). The results suggest that most major elements have no more than a 3% difference, and the largest difference is NiO, which is <15%. Hence, the uncertainty of mineral modal contents has only a minor effect on the reconstructed bulk rock compositions.

2.5. Mg isotope analysis of garnet and clinopyroxene

The mineral separates of clinopyroxene and garnet of samples from Obn eclogites were prepared for Mg isotope analysis. Individual grains (2–30 mg) used for isotope analysis were hand-picked under a binocular microscope in order to exclude pervasive alteration effects, such as serpentinization and kelyphitization. Both garnet and clinopyroxene without any visible lamellae or surface pitting were used. The separates were subjected to repeated (>3 times) ultrasonic cleaning in ultrapure water to eliminate any surface contamination. Isotopic ratios of Mg were

measured at the University of Science and Technology of China (USTC), following the procedures described in Huang et al (2011) and An and Huang (2014). Only a short summary is provided here. Total procedural blanks for Mg were less than 23 ng, which is insignificant relative to the amount of Mg (40 μg) put through chemical purification. Two standards (BCR-2 and BHVO-2) were measured for Mg isotope (expressed as $\delta^{26}Mg$ ($\delta^{26}Mg = 1{,}000*(^{26}Mg/^{24}Mg_{sample}/^{26}Mg/^{24}Mg_{standard}-1)$). The long term two standard deviation of $\delta^{26}Mg$ in the lab is less than 0.05‰. The $\delta^{26}Mg$ values of BCR-2 and BHVO-2 range from -0.154 to -0.125‰ and -0.188 to -0.195‰, respectively. These data show excellent agreement with literature values (-0.14 ± 0.11‰, Wombacher et al., 2009; -0.19 ± 0.09‰, Choi et al., 2012), highlighting the reliability of the Mg isotope data.

3. Results

3.1. Petrology and previous work

Nine fresh eclogites from the Obn kimberlite with high-MgO contents (reconstructed whole rock) were collected in this study. Fractures cross-cutting some samples contain penetrating kimberlitic and carbonate materials. Aside from these fractures, these samples are relatively fresh. Different from the Obn low-MgO eclogites containing only garnet and clinopyroxene (Sun et al., 2020), the Obn high-MgO eclogites contain discrete orthopyroxene grains and/or oriented orthopyroxene lamellae (up to 0.5 mm) in clinopyroxene in addition to the clinopyroxene and garnet. Garnets in the Obn high-MgO eclogites with pink color can be further divided into two types based on their textures. Coarse-grained Grts, which are subhedral to anhedral, have grain sizes ranging from 2–9 mm. Fine granular shaped Grt (<600 μm) inclusions are also found in Cpx. Clinopyroxenes with light to dark green are subhedral and up to 1 cm in size in most Obn high-MgO eclogites. Cpx with fine grain size (< 0.5 mm) enclosed by Grts also occur in a few samples. Accessory assemblages such as rutile, phlogopite, and sulfide occur in almost all the Obn high-MgO eclogites. Rutiles up to 20 μm occur as exsolutions in almost all garnets and clinopyroxenes. Phlogopites and sulfides are intergranular between Cpx and Opx. The detailed petrological description of Obn high-MgO eclogite is reported in the Supplementary Text A1. Eclogite and pyroxenite xenoliths from Obn have been investigated previously for their major and trace elements, and oxygen and Sr–Nd isotopes (Alifirova et al., 2012, 2015; Qi et al., 1994; Spengler and Alifirova, 2019; Sun et al., 2020; Sun et al., 2025; Taylor et al., 2003), the results of which are included and discussed in this study. Additionally, the Mg isotopes of minerals from the Obn low-MgO eclogites studied in Sun et al (2020) are also considered in this study.

3.2. Major and trace elements

Major and trace elements of Obn minerals are listed in Sup. Table A2 and Table A5, respectively. Major and trace elements of reconstructed whole rock values are listed in Table A6. Garnet grains of Obn high-MgO eclogites have MgO ranging from 17.0–22.2wt.% (Sup. Table A2). The coexisting clinopyroxene grains are mainly diopside in composition (Na_2O = 1.71–3.72 wt.%; Hills and Haggerty, 1989). Seven in nine samples in this study have a jadeite (Na/Na+Ca) component in clinopyroxene >0.2, indicating they are true eclogites (Clark et al., 1968).

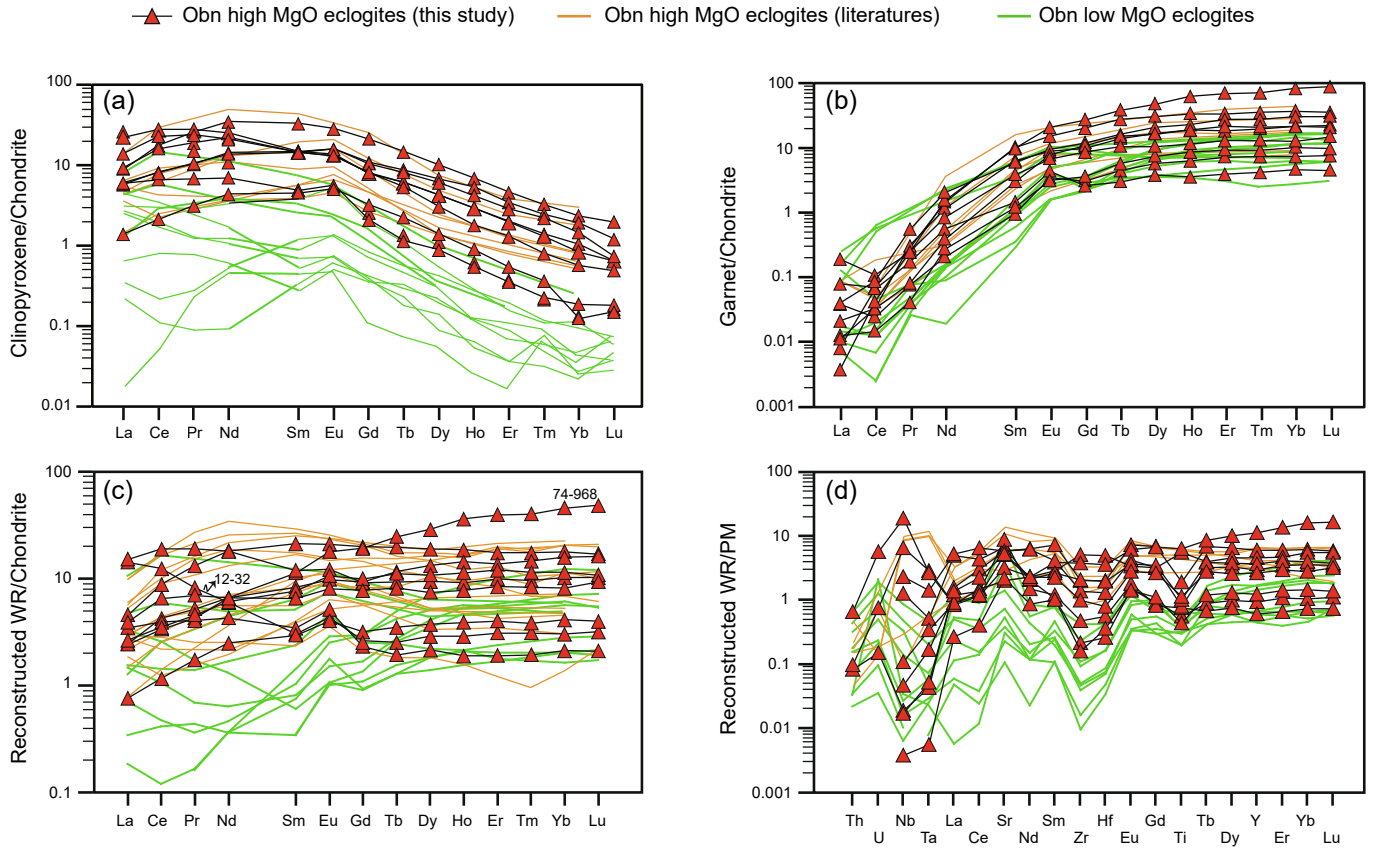

Fig. 1. (a) Chondrite-normalized REE patterns of clinopyroxenes from the Obnazhennaya high-MgO eclogites. (b) Chondrite-normalized REE patterns of coarse garnets from the Obnazhennaya high-MgO eclogites. (c) Chondrite-normalized reconstructed bulk REE concentrations of high-MgO eclogites estimated from the REE concentrations in minerals and their modes from Supplementary Table A2. (d) Primitive mantle-normalized reconstructed whole-rock trace element diagram for Obnazhennaya high-MgO eclogites. Orange lines are Obnazhennaya Group A or websterites from Qi et al (1994) and Taylor et al (2003). Green lines are Obnazhennaya low-MgO or Group B eclogites from Taylor et al (2003) and Sun et al (2020). Chondrite values and primitive mantle values are from McDonough and Sun (1995). The Ti, Zr, Hf, Nb and Ta contents in Fig. 1d are minima contents due to the clearness of rutile lamellae.

The other two samples Obn 12-27 and Obn 14-84 are classified as wehrlite since they have smaller jadeite components in clinopyroxene (0.14 and 0.15, respectively) as well as orthopyroxene. Both clinopyroxene and garnet have slightly positive Eu anomalies (δEu =Eu/SQRT (Sm*Gd)) or none (Fig. 1). Orthopyroxene grains have chemical compositions that vary with the microtexture of the eclogite, with orthopyroxene lamellae in clinopyroxene having higher Al_2O_3 and lower MgO contents than coarse grains. Both clinopyroxene and orthopyroxene have high Mg# (molar Mg/(Mg+Fe total)*100; 87.3–96.0 and 86.2–95.1 respectively). The estimated Mg# for bulk whole rock compositions ranges from 77.1–90.9 (Table A6). All reconstructed whole rock samples have flat to positively-sloped heavy rare earth elements (HREE) and positive Eu anomalies or none (Eu/Eu* range from 1.0–1.8; Table A6; Fig. 1). The Ti, Zr, Hf, Nb, and Ta contents (Table A6; Fig. 1d) represent minima values in eclogites due to the unclear volumes of rutile.

3.3. Mineral $\delta^{18}O$ and $\delta^{26}Mg$ isotopes

Oxygen isotopes of garnet for high-MgO eclogite, and magnesium isotopes of clinopyroxene and garnet grains for low-MgO eclogite and high-MgO eclogite are provided in Table 1 and Table A7, respectively. Garnet $\delta^{18}O$ for Obn high-MgO eclogite ranges from +5.18–+6.39‰, which is consistent with previous data for Obn high-MgO eclogites (+5.46–+6.46‰; Taylor et al., 2003), but the range is narrower than that of Obn low-MgO eclogite (+4.73‰–+7.8‰; Fig. 2a). Garnet $\delta^{26}Mg$ values range from -1.86‰ to -0.73‰ in Obn high-MgO eclogite, and from -1.09‰ to -0.55‰ in the Obn low-MgO eclogite (Fig. 2b). Clinopyroxene $\delta^{26}Mg$ values range from -1.13‰ to -0.08‰ in the Obn high-MgO eclogite, and from -0.33‰ to +0.01‰ in Obn low-MgO eclogite (Fig. 2b). The $\delta^{26}Mg$ values of garnet and clinopyroxene are strongly positively correlated (r^2 = 0.97 for high-MgO eclogite) and fall on equilibrium fractionation lines corresponding to temperatures of 900–1,350℃ (Fig. 2b).

Due to the small size of our rock samples, we could not conduct both whole-rock and separated-grains analyses. As such, we preferred the latter because the eclogite whole rocks are typically contaminated by kimberlite. Considering most orthopyroxene is present as lamellae of clinopyroxene, we can assume they are too small to significantly affect the bulk $\delta^{26}Mg$. The bulk $\delta^{26}Mg$ values calculated from the garnet and clinopyroxene data and weighted by the measured mineral models range from -1.47‰ to -0.36‰ in Obn high-MgO eclogite and from -0.76‰ to -0.27‰ in Obn low-MgO eclogite (Fig. 2c).

Table 1
Oxygen-isotope composition ($\delta^{18}O_{VSMOW}$‰) of garnets from high-MgO Obnazhennaya eclogites.

Sample	$\delta^{18}O_{VSMOW}$‰	2SD
This study		
7-359	6.11	0.28
12-27	5.24	0.30
12-32	5.25	0.34
12-68	5.41	0.30
14-83	5.38	0.34
14-84	5.18	0.30
14-91	6.07	0.30
14-95	5.30	0.42
74-968	6.39	0.32
Previous study		
O-4	6.35	0.52
O-926	5.60	0.14
O-901	5.79	0.62
O-423	6.07	0.17
O-1073	6.46	0.27
O-1109	6.14	0.28
O-1103	6.36	0.12
O-86/91	6.30	0.16
O-85/91	5.51	0.23
O-84/91	5.68	0.32
O-83/91	5.46	0.21
O-81/91	5.67	0.34
SMOW standard mean ocean water		
Previous studies are from Taylor et al. (2003).		

4. Discussion

4.1. Potential origins of high-MgO eclogite

4.1.1. Metasomatism

Metasomatism can lead to patent, cryptic, and/or stealth effects (O'Reilly and Griffin, 2013). The most commonly described examples of patent metasomatism in eclogite or pyroxenite xenoliths are the addition of amphibole, phlogopite, apatite, zircon, and/or carbonate and diamond (Aulbach et al., 2020a and references therein). Rutile or sulfide may also be the results of patent mantle metasomatism. The majority of Obn samples contain rutile (Sun et al., 2022) and phlogopite with both discrete grains and/or lamellae in clinopyroxene. It was suggested in previous studies that any process involving a change in pressure and/or temperature may produce exsolution lamellae, whereas the discrete phlogopite grains are the strongest evidence for metasomatism in the Obn samples. Additionally, metasomatic agents also cause significant changes in trace elements, especially in clinopyroxene, which leads to the LREE enrichment accompanied by the higher Sr contents and $(La/Yb)_N$ ratios. Obn high-MgO eclogites have enriched LREE (Fig. 1c), Sr content, and large $(La/Yb)_N$ ratios in clinopyroxene, characteristics which are all consistent with the Obn high-MgO eclogites having undergone metasomatism.

The origin of the metasomatic melt/fluid is speculative, but some possible agents include Mg-bearing melt/fluid derived from CO_2-rich fluids (Brenot et al., 2008; Higgins and Schrag, 2010; Ling et al., 2011; Tipper et al., 2006; Young and Galy, 2004) and/or mantle metasomatism melt such as kimberlite-like and ultramafic (UM) carbonated melts (Aulbach et al., 2020a). Additionally, based on melting model calculations, the Obn low-MgO eclogites underwent continuous partial melting at high pressures (Sun et al., 2020), thus the resulting melt from such a process may also be the metasomatic agent to further metasomatize the Obn high-MgO eclogites. Mg-bearing fluids can be ruled out because of their very low MgO contents (Xiao et al., 2013). Although serpentinite-derived fluids may have relatively high MgO content (Chen et al., 2023; Hu et al., 2020; Qiao et al., 2025), their MgO contents are <16% (Chen et al., 2016), which is far from the Obn high-MgO eclogites (>16%). Mantle metasomatism could form pyroxene via melt-rock reaction, and add to the modal contents of pyroxene in eclogites, which could have simultaneously increased bulk-rock MgO and SiO_2, and decreased Al_2O_3 contents of Obn high-MgO eclogites, leading to the correlation between MgO and other major elements. Moreover, mantle metasomatism could also reduce the jadeite component in clinopyroxene and increase the diopside contents, causing "pyroxenitisation" (Aulbach et al., 2020a). For example, Obn samples 12-27 and 14-84 are too omphacite-poor to be eclogites. Such changes can be explained by the addition of high-temperature pyroxene from an external kimberlite-like or UM carbonated melt (Aulbach et al., 2019, 2020; Mallik and Dasgupta, 2013).

4.1.2. Oxygen isotopes

Oxygen isotope compositions of mantle eclogites are commonly interpreted as reflecting seawater alteration on protoliths. Higher and lower $\delta^{18}O$ are the results of low- and high-temperature seawater alteration, respectively (Korolev et al., 2018). Although Riches et al (2016) and Korolev et al (2018) concluded that the metasomatism effect on $\delta^{18}O$ is not detectible, mass balance requires high fluid/melt-rock ratios to change the isotopic composition of the major element O (Radu et al., 2019). For example, Huang et al (2014) see evidence for an increase in $\delta^{18}O$ in response to mantle metasomatism in eclogites from Roberts Victor in South Africa. Kimberlite-like or UM carbonated melt

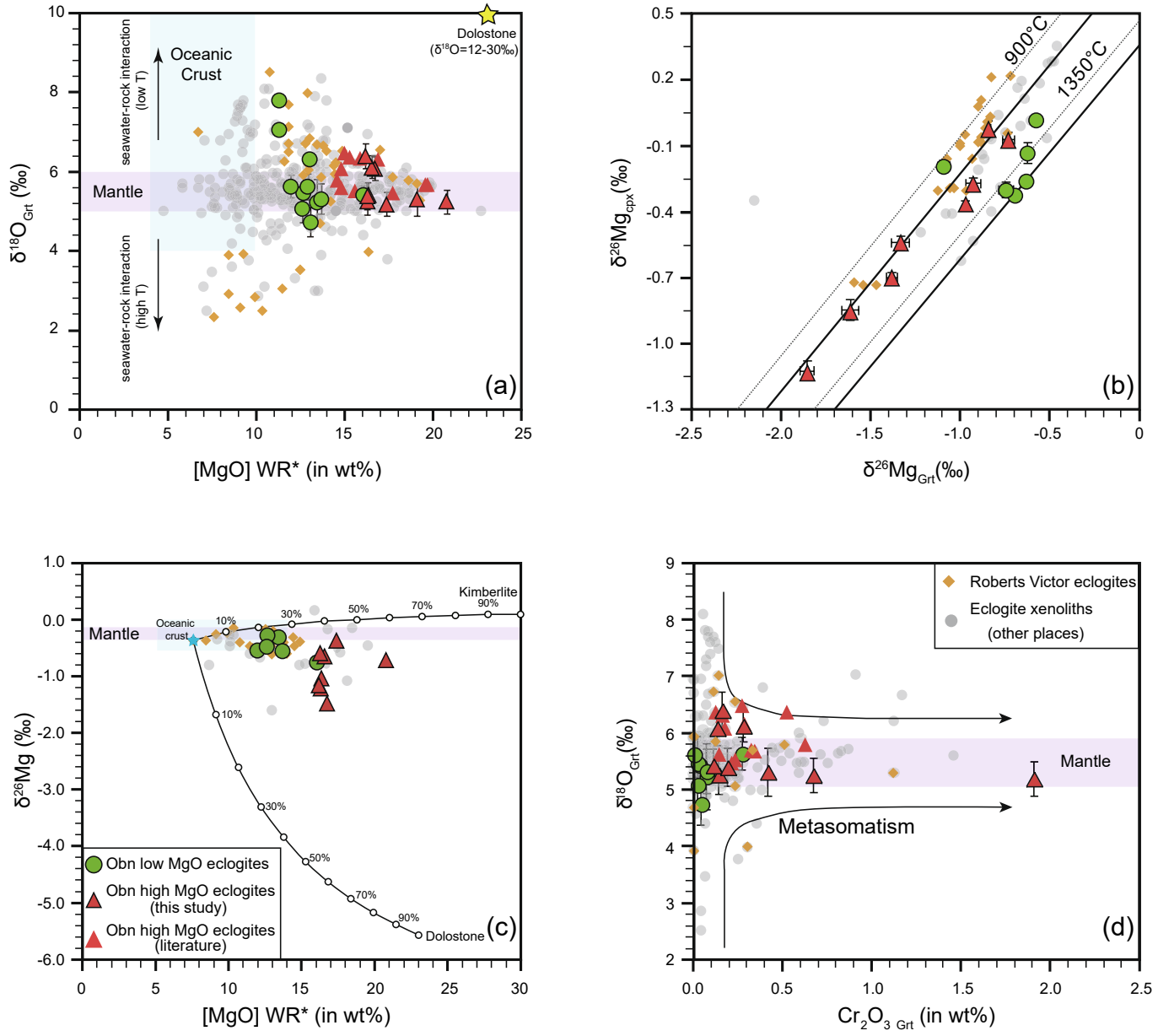

Fig. 2. (a) Garnet $\delta^{18}O$ values as function of eclogites MgO contents of reconstructed whole-rock compositions. (b) $\delta^{26}Mg_{grt}$ (garnet) versus $\delta^{26}Mg_{cpx}$ (clinopyroxene) for eclogites. (c) Calculated bulk rock $\delta^{26}Mg$ values as function of eclogites MgO contents of reconstructed whole-rock compositions. (d) Garnet $\delta^{18}O$ values versus garnet Cr_2O_3 contents. MgO contents of bulk rock is calculated based on mineral abundance and compositions of low-MgO eclogite and high-MgO eclogite, with data from Taylor et al (2003), Sun et al (2020), and this study. Equilibrium Mg isotope fractionations for different temperatures are calculated from Huang et al (2013), assuming pressures of 1 GPa (dashed line) and 6 GPa (solid line). Light purple and blue bars represent $\delta^{26}Mg$ and $\delta^{18}O$ values of normal mantle (Mattey et al., 1994; Teng et al., 2010) and oceanic crust (Eom et al., 2022; Gregory & Taylor, 1981), respectively. $\delta^{26}Mg$ and $\delta^{18}O$ values of dolostone are from Wang et al (2014) and Liu et al (2006). Orange diamonds and gray circles represent eclogites from the Roberts Victor kimberlite, and other places globally in Table A8. Blue star in (c) is gabbro from Oman oceanic crust with 7.6% MgO and -0.36‰ $\delta^{26}Mg$ (Eom et al., 2022). Dolostone with 23 wt.% MgO and -5.57‰ $\delta^{26}Mg$ (Teng, 2017). We assumed that kimberlite has 30 wt.% MgO contents and the same $\delta^{26}Mg$ as carbonatite (+0.1‰, Li et al., 2016).

metasomatism before or after subducted oceanic crust metamorphosed to eclogite is accompanied by an increase in Cr_2O_3 in both clinopyroxene and garnet (Fig. 3a in Aulbach et al., 2020a), hence Cr_2O_3 in garnet can be regarded as a proxy for the degree of metasomatic alteration. Statistically, then, the $\delta^{18}O$ of eclogites is mantle-like at high metasomatic intensity, because garnet from intensive metasomatized eclogites with high Cr_2O_3 values have mantle-like oxygen isotope signatures in the mantle (Aulbach et al., 2020a). Similarly, Czas et al (2018) also conclude that O isotopes can be modified at high melt/rock ratios, but only toward, and not away from, mantle values. The Obn high-MgO eclogites also plot in the range of existing data and fit the metasomatism range (Fig. 2d). We note that the garnet (obn14-84) with the highest Cr_2O_3 content (1.92%) has mantle-like $\delta^{18}O$ (+5.18‰). Moreover, we also observe that the oxygen isotope of garnets range toward the mantle values as well as increasing La in clinopyroxene (Fig. 3a). Hence, the mantle-like $\delta^{18}O$ values in Obn high-MgO eclogites could be the result of mantle metasomatism before or after subducted oceanic crust metamorphosed to eclogite. On the other hand, the initial $\delta^{18}O$ value of subducted oceanic crust is unknown due to low- and high-temperature seawater alteration; hence, the mantle-like $\delta^{18}O$ values of Obn high-MgO eclogites could also be a result of mixing.

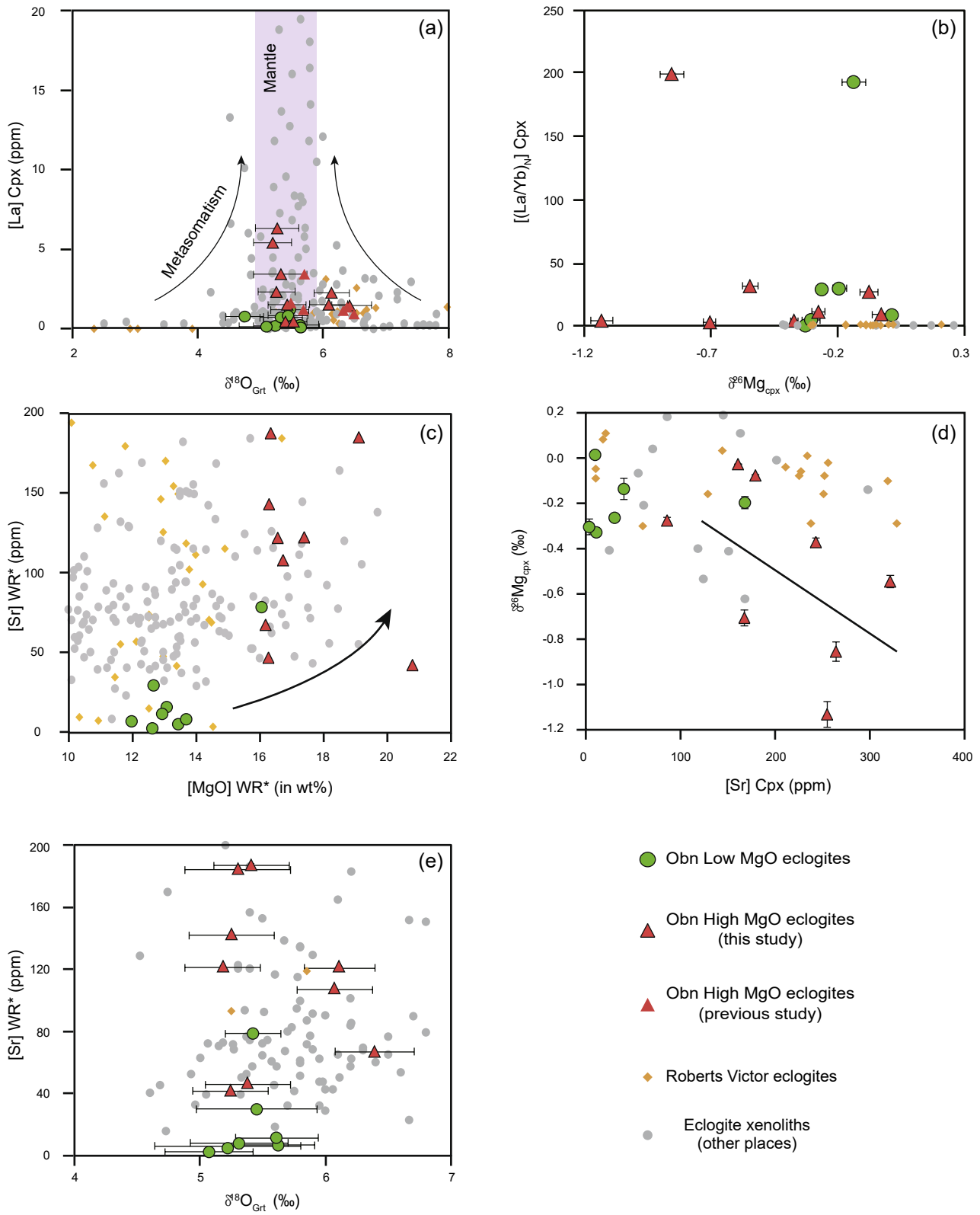

Fig. 3. (**a**) $\delta^{18}O$ of garnet versus indices of metasomatism (La of clinopyroxene). (**b**) $\delta^{26}Mg$ of clinopyroxene versus indices of metasomatism ($(La/Yb)_N$ of clinopyroxene). (**c**) MgO contents of reconstructed whole-rock composition as function of Sr contents. (**d**) Correlations between $\delta^{26}Mg$ of clinopyroxene versus Sr contents of clinopyroxene. (**e**) $\delta^{18}O$ of garnet versus Sr contents of whole rock. cpx: clinopyroxene; grt: garnet; WR*: reconstructed whole rock. Orange diamonds and gray circles represent eclogites from the Roberts Victor kimberlite, and other places globally in Table A8. The purple field depicts the oxygen isotope range of normal mantle (Mattey et al., 1994).

4.1.3. Origin of high-MgO Obn eclogite

Our new data for eclogite xenoliths from the Obn kimberlite pipe exhibiting a wide range of Mg contents provide a critical test of competing interpretations for the origins of mantle eclogite, particularly for high-MgO eclogite. Obn low-MgO eclogite has long been attributed to ancient (e.g., Obn eclogites were formed at around 1.2 Ga; Taylor et al., 2003) subducted oceanic crust (Sun et al., 2020; Taylor et al., 2003), which exhibits low δ^{26}Mg values. The δ^{26}Mg isotope values of garnet, clinopyroxene, and the reconstructed whole-rock compositions of the low-MgO eclogite in this study plots in range of altered oceanic crust (Fig. 2b and c), further supporting this hypothesis.

For Obn high-MgO eclogite, the strong Eu anomaly in garnet, clinopyroxene, and reconstructed whole-rock compositions suggest a plagioclase-rich protolith that formed at low pressure. Together with the heavier oxygen isotopes that suggest the influence of seawater alteration, and the light Mg values that may show the contribution of crustal materials, we can rule out a high-pressure mantle cumulate origin (Hills and Haggerty, 1989). Reaction products due to element exchange between low-MgO eclogite and surrounding peridotites have been proposed for shallow eclogites of the Koidu (Wang et al., 2015) and Jericho

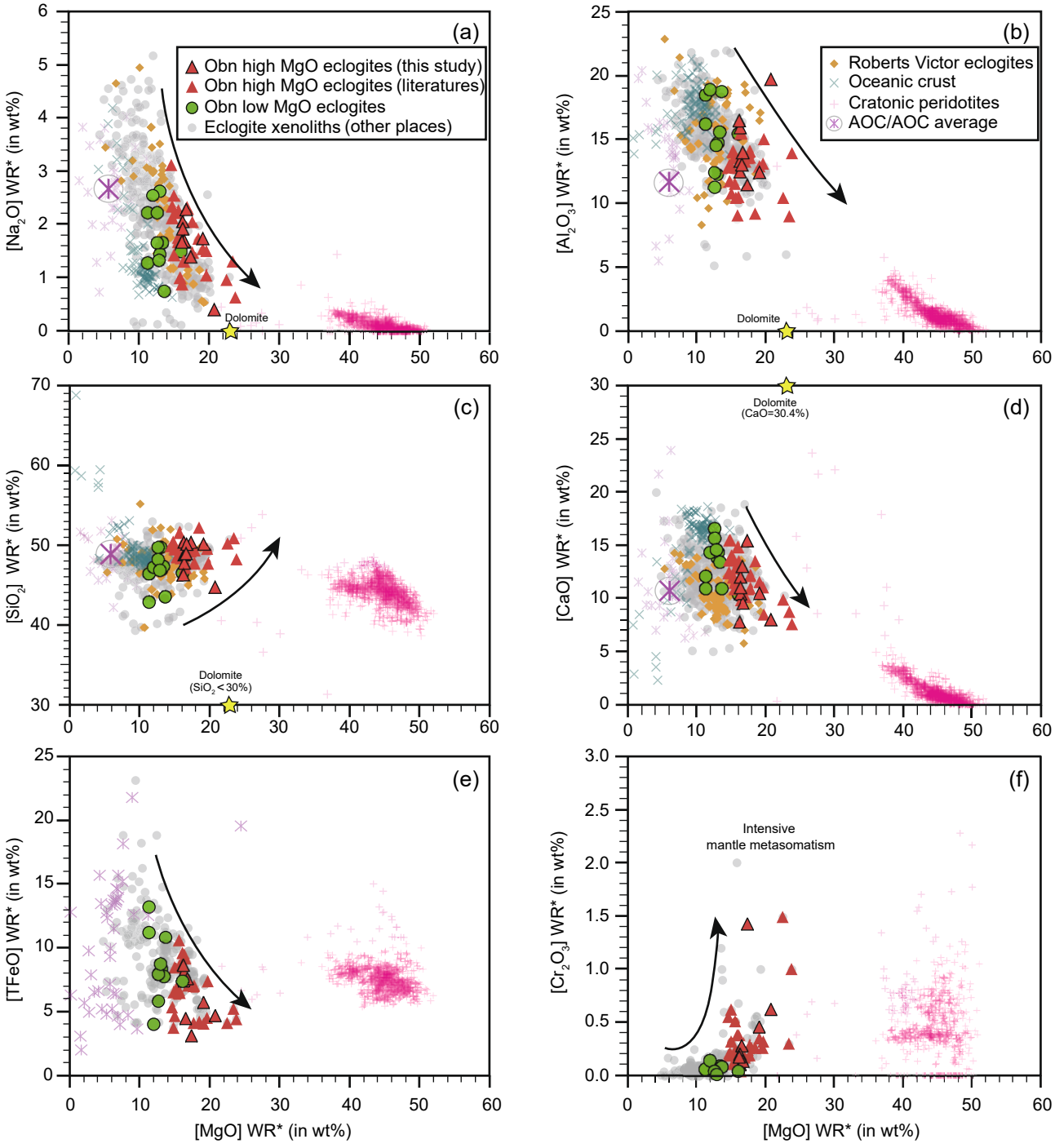

Fig. 4. MgO contents as function of Na_2O (a), Al_2O_3 (b), SiO_2 (c), CaO (d), TFeO (e), and Cr_2O_3 (f) contents of reconstructed whole-rock composition. Bulk major element compositions are calculated based on mineral abundance and composition. Green circles are low-MgO eclogite and Group B eclogites. Obn Group A or high-MgO eclogites are from the literature. Altered oceanic crust (AOC) data and average AOC are from Li et al (2007). Oceanic crust data are from Garbe-Schönberg et al (2022). All data and references are provided in Table A8.

(Smart et al., 2009) kimberlites. Eclogite in the lithospheric mantle has a lower solidus temperature than the surrounding peridotite, making it melt before peridotite, thus generating melts that facilitate element exchange between restitic eclogite and peridotite by rapid diffusion (Wang et al., 2015). The high-MgO and low Na_2O and Al_2O_3 contents (Fig. 4a-b) of Obn high-MgO eclogite may result from elemental diffusion between Obn low-MgO eclogite and peridotite. However, if element exchange between low-MgO eclogite and peridotite occurred, the SiO_2 (Fig. 4c) contents should plot in between the low-MgO eclogite and peridotites, which is inconsistent with our observations. Obn high-MgO eclogite has similar or higher SiO_2 contents compared with both Obn low-MgO eclogites and peridotites (Fig. 4c). Hence, the melt-diffusion hypothesis cannot explain the origin of Obn high-MgO eclogite.

The more likely origin of Obn high-MgO eclogite is subducted oceanic crust modified by mantle metasomatism, as proposed by Aulbach et al. (2020a). The Eu anomaly in reconstructed whole-rock and heavier oxygen isotope in some Obn high-MgO eclogites suggests that the Obn high-MgO eclogites have oceanic crust as a protolith. Orthopyroxene existing exclusively in high-MgO eclogite may be because of their protoliths represent a different part of oceanic crust. For example, the lower part of oceanic crust consisting of gabbro-norite or norite contains orthopyroxene before it gets subducted. After the ancient oceanic crust gets subducted beneath the lithospheric mantle, it may suffer metamorphism, mantle metasomatism (kimberlite-like and UM carbonated melt) prior to its entrainment in kimberlite, which may change its composition significantly. Both the petrological characteristics and metasomatic tracers (i.e., LREE) in Obn high-MgO eclogite suggest some of these eclogites were mantle metasomatized. Mantle metasomatism enriched the LREE contents in both bulk-rock and clinopyroxene, as well as increasing the MgO and SiO_2 content, and decreasing the bulk rock Na_2O, Al_2O_3, CaO, and TFeO (Fig. 4) through the addition of high-temperature clinopyroxene. Another hallmark of mantle metasomatism is a lower jadeite component in clinopyroxene, which can cause "pyroxenitization", such as samples obn12-27 and obn14-84. Moreover, mantle metasomatism also results in the mantle-like oxygen isotopic values of Obn high-MgO eclogites as well as increased Cr_2O_3 in garnet. Samples 12-27 and 14-84 with low jadeite contents (0.14 vs. 0.15) have the highest Cr_2O_3 (0.68% vs. 1.92%) and mantle-like $\delta^{18}O$ (5.24‰ vs. 5.18‰), supporting this hypothesis. However, mantle metasomatism cannot explain the light and heterogeneous Mg isotopes of the Obn high-MgO eclogites. Although there are no Mg isotope data for kimberlite available, both the kimberlite and ultramafic carbonated melt may have mantle-like Mg isotopes, which are heavier than those of Obn high-MgO eclogites. A simple bulk mixing calculation between oceanic crust and kimberlite, assuming the kimberlite has the same Mg isotope value as carbonatite (-0.3‰–+0.37‰; Li et al., 2016), suggests the kimberlitic magma can only increase the MgO contents (Fig. 2c). No correlation between $(La/Yb)_N$ and $\delta^{26}Mg$ in clinopyroxene (Fig. 3b) also indicates that mantle metasomatism did not affect the Mg isotopic composition of Obn high-MgO eclogites. Kinetic Mg isotope fractionation could occur during mantle metasomatism increasing eclogite MgO contents. The colder oceanic crust of the downgoing plate relative to the surrounding lithospheric peridotite would provide a strong thermal gradient that might enhance the diffusion of ^{24}Mg from the relatively hot peridotite to the cold oceanic crust (plus sediments), as light isotopes diffuse faster than heavy isotopes (Richter et al., 2009). The mantle metasomatic melt is removed before the isotopic composition gets reset back to "normal" composition and an isotopically light signature could be preserved. Similar scenarios can be found in Ca–Fe isotopes (Zhao et al., 2017). Model calculations suggest that the extremely light Ca–Fe isotopic signatures in peridotites are the result of kinetic isotopic fractionation during melt-peridotite reaction spanning 10^4 years. Xiao et al (2013) also suggests that light and disequilibrium Mg isotope signatures (+0.09 to -0.39‰) in Cr-peridotites can be attributable to kinetic isotope fractionation during incomplete melt-peridotite refraction. Therefore, the light Mg isotopic compositions of Obn high-MgO eclogites could be the result of kinetic isotope fractionation during mantle metasomatism. Alternatively, the light Mg isotopic compositions in high-MgO eclogites may be due to the involvement of carbonate sediment. Carbonate and pelagic sediments are widespread on the seafloor and therefore may be potentially incorporated during subduction at the interface between the downgoing oceanic slab and the overlying lithospheric mantle. Carbonates and pelagic sediments have notably low $\delta^{26}Mg$ isotopic compositions, ranging from -5.57‰ to -1.09‰ (Brenot et al., 2008; Higgins and Schrag, 2010; Hippler et al., 2009; Pogge von Strandmann, 2008; Teng, 2017; Tipper et al., 2006; Young and Galy, 2004). As such, a few carbonate and pelagic sediments on the oceanic crust would lead to light Mg isotopic composition. Additionally, Sr is a proxy for carbonates and pelagic sediments, where the more carbonate addition, the higher the Sr contents in eclogites. The Obn high-MgO eclogites contain 3–8 times the Sr contents of the Obn low-MgO eclogites, and there is a negative correlation between $\delta^{26}Mg$ values and Sr contents in clinopyroxene (Fig. 3d). All these characteristics suggest the involvement of carbonate and pelagic sediments is the reason for light Mg isotopic compositions of high MgO eclogites. Both mantle metasomatism (kimberlitic like or ultramafic carbonated melt) and carbonate or pelagic sediments involvement can increase the Sr contents in eclogites, and the lack of correlation between MgO and Sr contents (Fig. 3c) suggest that the carbonate sediments involvement have less effect on MgO contents. Similarly, the lack of a correlation between Sr content and $\delta^{18}O$ suggests that the carbonate addition did not change the oxygen isotopes of the Obn high-MgO eclogites (Fig. 3e). Alternatively, mixing among the mantle metasomatism, carbonate sediments involvement, and subducted oceanic crust could also lead to the mantle-like oxygen isotopes.

Thus, we finally consider whether subducted oceanic crust modified by mantle metasomatism and the potentially critical addition of carbonate sediment may more completely represent the collective protoliths of the Obn high-MgO eclogites—specifically, ancient oceanic crust with carbonate sediment subducted into the mantle and metamorphosed to eclogite. Also, kimberlite-like or UM carbonated melt metasomatized the subducted oceanic crust or eclogites when they were stored in the lithospheric mantle. Before evaluating the aforementioned hypothesis, a bulk-mixing calculation between dolostone and oceanic crust was used to evaluate the hypothesis of a combined protolith of oceanic crust (without metasomatism) plus Mg-rich carbonate sediments. Dolostone, Mg-rich sedimentary carbonate, has higher MgO contents (23 wt.%) but lower $\delta^{26}Mg$ (-5.57‰; Teng, 2017). The calculations suggest that >50% dolostone by mass (Fig. 2c) is needed to account for both high-MgO contents with no kimberlitic melt metasomatism, which is unrealistically high for natural settings. Therefore, the most possible protolith of Obn high-MgO eclogites is oceanic crust subducted into the mantle with the involvement of carbonate sediments and mantle metasomatism. To determine if this hypothesis accounts for the O–Mg isotopic composition (Fig. 5) and MgO–$\delta^{26}Mg$ (Fig. 2c) of our samples, we model ternary mixing scenario among carbonate sediments, kimberlitic melt and oceanic crust. The bulk mixing calculation suggests that oceanic crust modified by kimberlite-like melt metasomatism as well as no more than 10% carbonate sediments involvement can explain the MgO contents and Mg and oxygen isotopic compositions of all Obn high-MgO eclogites. Meanwhile, this model can also explain the lower jadeite component in clinopyroxene and higher diopside contents in Obn high-MgO eclogites.

4.2. Global test: Carbonates as a missing ingredient in the formation of mantle eclogites?

In order to test whether our preferred "just add carbonates" recipe for mantle eclogites that can account for our new data from Siberia craton is globally representative, we compiled a comprehensive global dataset of mantle eclogite xenoliths from 23 kimberlite pipes from around the world (Table A8). Similar to the clear distinction between

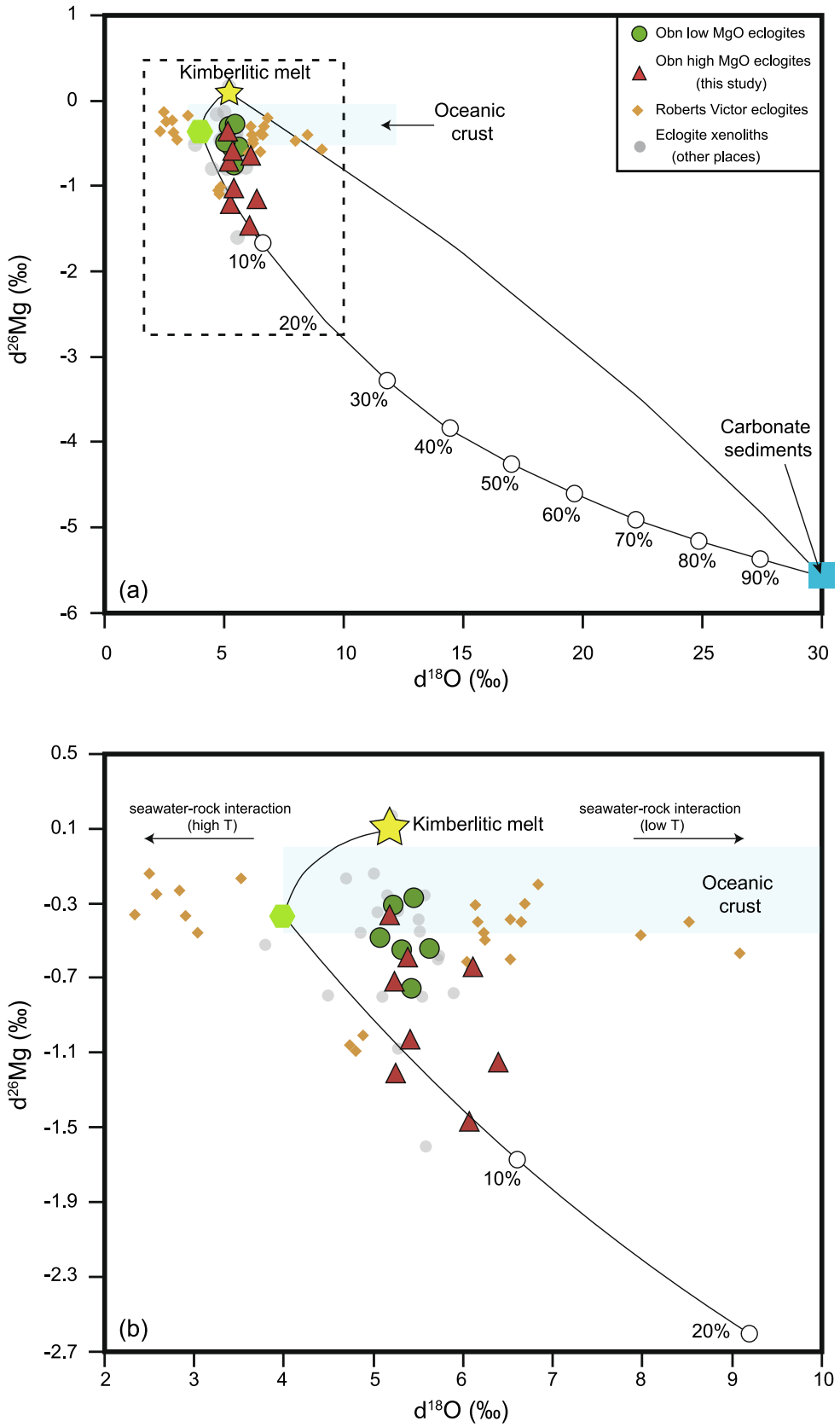

Fig. 5. Mg–O isotopic mixing among oceanic crust, kimberlitic melt, and carbonate sediments. We assume that carbonate sediment (blue square) has 23% MgO, with $\delta^{18}O$ and $\delta^{26}Mg$ values of +30‰ (Liu et al., 2006) and -5.57‰ (Teng, 2017), respectively. Kimberlite (yellow star) has 30% MgO contents and the same $\delta^{26}Mg$ as carbonatite (+0.1‰, Li et al., 2016) with $\delta^{18}O$ (+5.18‰; Xu et al., 2021). The green hexagon represents oceanic crust with 7.67% MgO, +4‰ $\delta^{18}O$, and -0.36‰ $\delta^{26}Mg$. The light blue area represents $\delta^{18}O$ (Gregory and Taylor, 1981) and $\delta^{26}Mg$ (Eom et al., 2022) of Oceanic crust. Data for other eclogites and their references are provided in Table A8.

low-MgO eclogite and high-MgO eclogite in our Obn case study (Fig. A1), as in many such case studies of individual kimberlite pipes in previous work (e.g., Aulbach et al., 2019), such a distinction is also evident in the global dataset. Notably, whereas the whole rock SiO_2, CaO, and Al_2O_3 contents are unimodal (Fig. A1a-c), the MgO of whole rock (Fig. 6a) and MgO contents in clinopyroxene and garnet of eclogites (Fig. 6b-c) globally yield *bimodal* distributions, providing a global and statistical basis for regarding low-MgO eclogite and high-MgO eclogite as distinct "groups" as traditionally done. Thus, in light of the fact that our preferred model for our new regional data is indeed globally representative, we tentatively extend this "just add carbonates" recipe for the origin of mantle eclogites more generally.

Most if not all existing studies suggests that the protolith of all mantle eclogites is subducted oceanic crust, with the only difference proposed here being that eclogites with higher MgO contents suffered mantle metasomatism and the addition of carbonate sediment (Fig. 7). Ternary mixing scenario among carbonate sediments, kimberlitic melt and oceanic crust and its effects on O–Mg isotopic compositions (Fig. 5) and MgO-δ^{26}Mg (Fig. 2c) suggests that most global eclogite xenoliths require the addition of carbonate sediments, although there are relatively less Mg and O isotopic compositions of eclogites reported so far. The mantle metasomatism can be regarded as being responsible for the decreased jadeite component in clinopyroxene, decreased TFeO, Al_2O_3, and Na_2O in bulk rock, and increased bulk-rock MgO, SiO_2, and Cr_2O_3, thus leading to the negative correlations with whole-rock MgO (Fig. 4). The mantle metasomatism can also account for the mantle-like range of $\delta^{18}O$ of high-MgO eclogite (Aulbach et al., 2020a). The higher MgO (Fig. 2a) and La contents (Fig. 3a), the closer the $\delta^{18}O$ of garnet in eclogites would be to mantle values. On the other hand, the low-MgO eclogites have wider $\delta^{18}O$ range, suggesting that they underwent hydrothermal alteration at variable temperatures. The significantly lower $\delta^{18}O$ values than that of present-day oceanic crust might be due to a combination of the lower $\delta^{18}O$ (-10‰) of seawater in the Precambrian and/or a higher temperature of seawater-oceanic crust interaction (Radu et al., 2019). In global eclogite xenoliths, the higher the MgO contents in bulk rock, the lighter and more heterogeneous the δ^{26}Mg values (Fig. 2c). This could be because of the kinetic fractionation during metasomatism or the additional melting of carbonate sediment in the lithospheric mantle. Evidence for subducted carbonate transported into Earth's deep mantle has been identified in ocean island basalt with high δ^{66}Zn and light δ^{26}Mg (Wang et al., 2018; Zhang et al., 2022). Mg-rich carbonate sediments (i.e., dolostone) is widespread throughout most of Earth's sedimentary rock record, particularly in protracted Precambrian time (Petrash et al., 2017), such as the Paleoproterozoic Postmasburg Group in South Africa (Beukes and Smit, 1987) and Lagoa Vermelh in Brazil (Meister et al., 2011). Li et al (2017) also suggested that partially dissolved Ca-rich carbonate sediments (dehydrated sediments) and undissolved Mg-rich carbonate sediments can be carried into the mantle separately during slab dehydration. We suggest that such a separation of Ca- and Mg-rich fluids and melts during slab dehydration and stagnation, in tandem with carbonate sediment with varying amounts of Ca/Mg content (i.e., limestone vs. dolostone), can collectively potentially explain why certain regions are dominated by either low- or high-MgO eclogites (Fig. 7). Thus, in light of our new results and in the context of our global compilation, we propose a general model for the origin of eclogite xenoliths that they formed from subducted oceanic crust with or without mantle metasomatism as well as the addition of carbonate sediment.

This unified view of mantle eclogites implies that the continental lithosphere is not only an archive of ancient subducted oceanic crust, but also an archive of ancient sediments. Because of this preservation, the ancient sediment records have not been entirely lost, and the diffusion of the chemical signatures of these subducted carbonates has been imprinted in mantle eclogites. This model—integrating a central role for subducted carbonates into mantle eclogite petrogenesis—can account for deep, carbonate-rich domains in the subcontinental lithospheric mantle (SCLM) (Foley and Fischer, 2017; Gorczyk and Gonzalez, 2019), which carries implications for the global carbon cycle and even potential climate change events when this deep lithospheric carbon reservoir gets later disrupted during continental rifting and intraplate magmatism (Gernon et al., 2022; Sobolev et al., 2011).

This hypothesis pointing to a potential explanation of eclogite xenoliths as subducted oceanic crust with the involvement of carbonate provides impetus for further testing as more and more Mg isotopic composition of eclogites are reported. Diamond—the most widely reported carbon mineral in eclogite, thus rendering cratonic eclogite a prime source for gem-quality diamonds—may offer a clue to pursue. If high-MgO eclogites are indeed the result of interaction with high-MgO carbonates, the question arises why little to no carbonate content is found in mantle eclogite and why high-MgO eclogites host less diamond than low-MgO eclogites from some kimberlite pipes, such as the

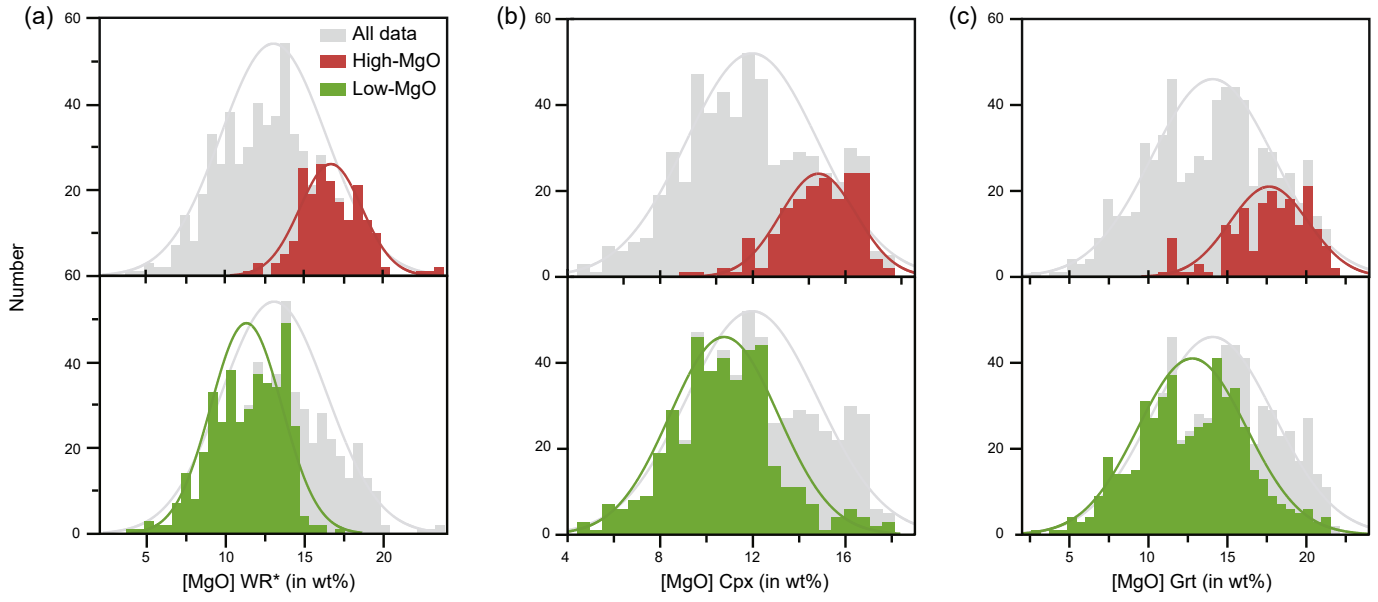

Fig. 6. Frequency histogram and probability density function MgO (**a**) contents of reconstructed whole rock, MgO contents of clinopyroxene (**b**) and garnet (**c**) in eclogites from this study and worldwide. Data and references are from Table A8. The grey histogram represents all data, and the green and red histograms represent low-MgO eclogite and high-MgO eclogite, respectively.

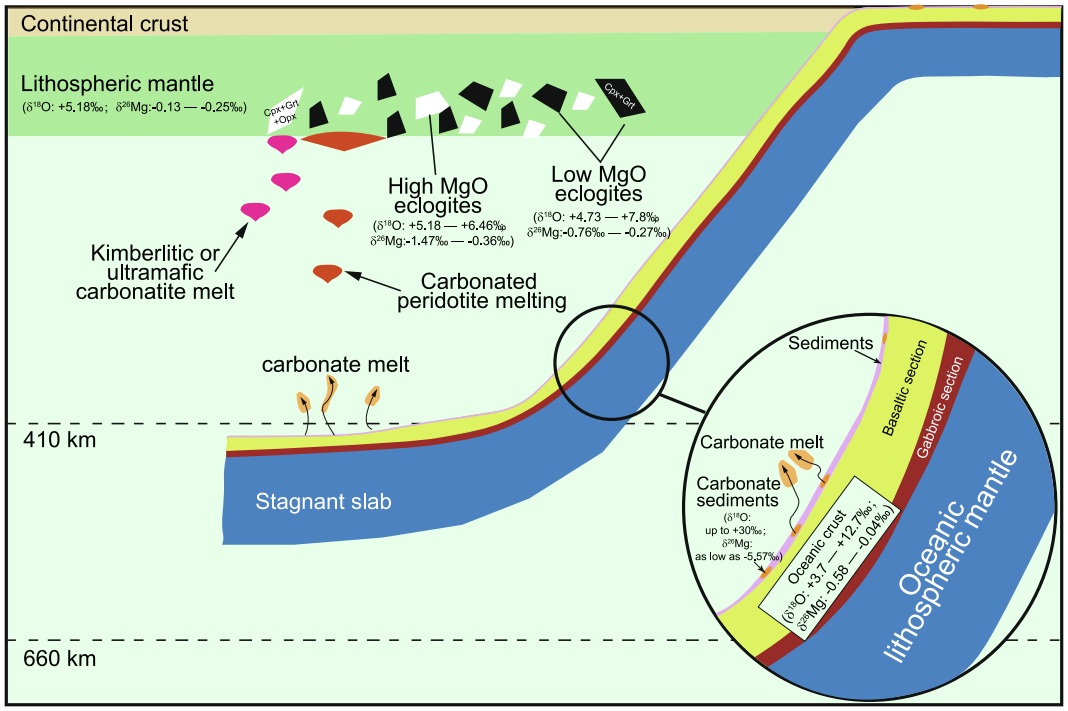

Fig. 7. Model for the formation of both low-MgO and high-MgO eclogites under the additional influence of carbonates with variable amounts of Mg content. The formation processes of high MgO eclogites are (1) oceanic crust with the involvement of carbonate sediments subducted into the mantle and metamorphismed to eclogites, with carbonate melt released during the subduction process; (2) kimberlitic or ultramafic carbonatite melt metasomatized the high-MgO eclogite before or after metamorphism. The low-MgO eclogites were formed at by the gabbroic section of subducted oceanic crust that underwent continued partial melting processes (Sun et al., 2020) without the involvement of carbonate sediments and kimberlitic or ultramafic carbonatite melt metasomatism. The $\delta^{18}O$ and $\delta^{26}Mg$ values of high-MgO and low-MgO eclogites were data of Obnazhenanya eclogites. The $\delta^{18}O$ and $\delta^{26}Mg$ values of lithospheric mantle, carbonate sediments and oceanic crust are from Mattey et al. (1994), Teng et al. (2010), Liu et al. (2006), Teng, (2017), Gregory & Taylor, (1981) and Eom et al. (2022).

Doornkloof-Sover and Newlands pipes from western Kaapvaal craton (Aulbach et al., 2020b). Given that the peridotite and the eclogite part of the deep SCLM is too reduced for carbonate to be stable (Aulbach et al., 2022; Stagno et al., 2013), it is typically assumed that most carbonate in diamond is not primary but secondary. The direct conversion of intrinsic carbon in oceanic crust is kinetically inhibited, so the influx of metasomatic fluids or melts is considered required for diamond growth (Stachel and Luth, 2015; Stachel et al., 2022). Traditionally then, they have/have-not nature of diamonds in low- and high-MgO eclogites, respectively, has been ascribed to the dominantly diamond-destructive effect of kimberlite-melt metasomatism that increases eclogite MgO content (Aulbach et al., 2019; Aulbach et al., 2020a, 2020b). However, it should also be noted that diamond is generally found in oxidized environments and not as often in reduced ones. Carbonates are an oxidizing component, so a large carbonate component might arguably prevent diamond from forming in the first place. So, if high-MgO eclogite forms via interaction with carbonates, then one should in fact not expect diamonds—with or without later mantle metasomatism. Thus, although diamonds are nonetheless found in some high-MgO eclogites, the fact that we did not find diamond in high-MgO eclogite xenoliths from Obn could be interpreted as being consistent with carbonate sediment being a missing ingredient in the diverse origins of mantle eclogite.

5. Conclusions

In this study, we analyzed major and trace elements of minerals, oxygen isotope of garnets of high MgO eclogites, and Mg isotope of clinopyroxene and garnets from both high and low MgO eclogites in Obn kimberlite, Siberia craton. We also reconstructed the whole rock major and trace elements and Mg isotopic compositions. All Obn high MgO eclogites have MgO ranging from 17.0–22.2wt.%, and flat to positively-sloped heavy rare earth elements (HREE) and positive Eu anomalies or none (Eu/Eu* range from 1.0–1.8). Garnet $\delta^{18}O$ for Obn high-MgO eclogite ranges from +5.18–+6.39‰. The bulk $\delta^{26}Mg$ values calculated from the garnet and clinopyroxene data and weighted by the measured mineral models range from -1.47‰ to -0.36‰ in Obn high-MgO eclogite and from -0.76‰ to -0.27‰ in Obn low-MgO eclogite. All these characteristics suggest the origin of Obn high-MgO eclogites is oceanic crust subducted into the mantle with the involvement of carbonated sediments, and then metasomatized by kimberlite-like or ultramafic carbonated melt. This model is also compatible with global mantle eclogite observations, where there is also a clear distinction between high- and low-MgO eclogites globally. In light of our new results and global compilation, we propose that mantle eclogites represent a spectrum of subducted oceanic crust with or without carbonate sediments.

CRediT authorship contribution statement

Jing Sun: Writing – review & editing, Writing – original draft, Conceptualization. **Ross N. Mitchell:** Writing – review & editing. **Luc S. Doucet:** Writing – review & editing. **Kouki Kitajima:** Methodology. **Ranpeng Li:** Data curation. **Jinglin Su:** Data curation. **Qiqi Ou:** Data curation. **Tanya Kalashnikova:** Conceptualization. **Sergey I. Kostrovitsky:** Conceptualization.

Declaration of competing interest

The authors declare that they have no known competing financial interests or personal relationships that could have appeared to influence the work reported in this paper.

Acknowledgments

This study was funded by the National Natural Science Foundation of China (42072060) and open fund of State Key Laboratory of Geological Processes and Mineral Resources, China University of Geosciences, Wuhan (Project No. GPMR202201). Additional support came from the President's International Fellowship Initiative (PIFI; 2021FYC0002) granted to Mitchell. Sun benefitted from continuous help and support in the laboratory and through discussions with John Valley and Michael Spicuzza (University of Wisconsin, SIMS), Francisco Apen, Gareth Seward, and Roberta Rudnick (University of California, Santa Barbara), Lihui Chen (Northwest University), Fang Huang (University of Science and Technology of China). An earlier version of the manuscript benefitted from detailed review comments from Shuijiong Wang, Sonja Aulbach and Nicholas Arndt.

Appendix A. Supplementary data

Supplementary data to this article can be found online at https://doi.org/10.1016/j.gr.2025.11.015.

References

Alifirova, T.A., Pokhilenko, L.N., Ovchinnikov, Y.I., Donnelly, C.L., Amy, J.V.R., Taylor, L.A., 2012. Petrologic origin of exsolution textures in mantle minerals: evidence in pyroxenitic xenoliths from Yakutia kimberlites. Int. Geol. Rev. 54, 1071–1092. https://doi.org/10.1080/00206814.2011.623011.

Alifirova, T.A., Pokhilenko, L.N., Korsakov, A.V., 2015. Apatite, SiO_2, rutile and orthopyroxene precipitates in minerals of eclogite xenoliths from Yakutian kimberlites, Russia. Lithos 226, 31–49. https://doi.org/10.1016/j.lithos.2015.01.020.

An, Y.J., Huang, F., 2014. A review of Mg isotope analytical methods by MC-ICP-MS. J. Earth Sci. 25, 823–841. https://doi.org/10.1007/s12583-014-0477-8.

Armstrong, J.T., 1995. CITZAF-A package of correction programs for the quantitative electron microbeam X-ray-analysis of thick polished materials, thin-films, and particles. Microbeam Anal. 4, 177–200.

Aulbach, S., Stachel, T., Viljoen, S.K., Brey, G.P., Harris, J.W., 2002. Eclogitic and websteritic diamond sources beneath the Limpopo Belt-Is slab-melting the link? Contrib. Mineral. Petrol. 143 (1), 56–70. https://doi.org/10.1007/s00410-001-0331-8.

Aulbach, S., Pearson, N.J., O'Reilly, S.Y., Doyle, B., 2007. Origins of xenolithic eclogites and pyroxenites from the central Slave Craton. Canada. J. Petrol. 48 (10), 1843–1873. https://doi.org/10.1093/petrology/egm041.

Aulbach, S., Hofer, H.E., Gerdes, A., 2019. High-Mg and low-Mg mantle eclogites from Koidu (West African Craton) linked by Neoproterozoic ultramafic melt metasomatism of subducted Archaean plateau-like oceanic crust. J. Petrol. 60, 723–754. https://doi.org/10.1093/petrology/egz011.

Aulbach, S., Massuyeau, M., Garber, J.M., Gerdes, A., Heaman, L.M., Viljoen, K.S., 2020a. Ultramafic carbonated melt and auto metasomatism in mantle eclogites: Compositional effects and geophysical consequences. Geochem., Geophys., Geosyst. 21 (5), e2019GC008774. https://doi.org/10.1029/2019GC008774.

Aulbach, S., Viljoen, K.S., Gerdes, A., 2020b. Diamondiferous and barren eclogites and pyroxenites from the western Kaapvaal craton record subduction processes and mantle metasomatism, respectively. Lithos 368–369, 105588. https://doi.org/10.1016/j.lithos.2020.105588.

Aulbach, S., Woodland, A.B., Stango, V., Korsakov, A.V., Mikhailenko, D., Golovin, A.V., 2022. Fe^{3+} distribution of $Fe^{3+}/\sum$Fe-oxygen fugacity variations in kimberlite-borne eclogite xenoliths, with comments on clinopyroxene-garnet oxy-thermobarometry. J. Petrol. 63 (8). https://doi.org/10.1093/petrology/egac076.

Barth, M.G., Rudnick, R.L., Horn, I., McDonough, W.F., Spicuzza, M., Valley, J.W., Haggerty, S.E., 2001. Geochemistry of xenolithic eclogites from West Africa: Part I. A link between low MgO eclogites and Archean crust formation. Geochim. Cosmochim. Acta 65 (9), 1499–1527. https://doi.org/10.1016/S0016-7037(00)00626-8.

Barth, M.G., Rudnick, R.L., Horn, I., McDonough, W.F., Spicuzza, M.J., Valley, J.W., Haggerty, S.E., 2002. Geochemistry of xenolithic eclogites from West Africa, part 2: Origins of the high-MgO eclogites. Geochim. Cosmochim. Acta 66 (24), 4325–4345. https://doi.org/10.1016/S0016-7037(02)01004-9.

Berner, R.A., 2009. Phanerozoic atmospheric oxygen: new results using the geocarbsulf model. Am. J. Sci. 309 (7), 603–606. https://doi.org/10.2475/07.2009.03.

Beukes, N.J., Smit, C.A., 1987. New evidence for thrust faulting in Griqualand West, South Africa: implications for stratigraphy and the age of red beds. S. Afr. J. Geol. 90 (4), 378–394.

Brenot, A., Cloquet, C., Vigier, N., Carignan, J., France-Lanord, C.F., 2008. Magnesium isotope systematics of the lithologically varied Moselle River basin. France. Geochim. Cosmochim. Acta 72 (20), 5070–5089. https://doi.org/10.1016/j.gca.2008.07.027.

Chen, C.F., Liu, X.G., Hu, Z.C., Zong, K.Q., Liu, Y.S., 2014. In situ analysis of major and trace element compositions of hydrous silicate minerals by LA-ICP-MS. J. Earth Sci. 39, 525–536. https://doi.org/10.3799/dqkx.2014.050.

Chen, Y.X., Schertl, H.P., Zheng, Y.F., Huang, F., Zhou, K., Gong, Y.Z., 2016. Mg-O isotopes trace the origin of Mg-rich fluids in the deeply subducted continental crust of Western Alps. Earth Planet. Sci. Lett. 157–167. https://doi.org/10.1016/j.epsl.2016.09.010.

Chen, A.X., Chen, Y.X., Gu, X.F., Zeng, Z., Xiao, Z.C., Schertl, H.P., Han, X.Q., Zhao, Z.F., Huang, F., 2023. Barium isotope behavior during interaction between serpentinite-derivd fluids and metamorphic rocks in the continental subduction zone. Geochim. Cosmochim. Acta 353, 61–75.

Choi, M.S., Ryu, J.S., Lee, S.W., Shin, H.S., Lee, K.S., 2012. A revisited method for Mg purification and isotope analysis using Cool-Plasma MC-ICP-MS. J. Anal. At. Spectrom. 27 (11), 1955–1959. https://doi.org/10.1039/c2ja30191a.

Clark, J.R., Appleman, D.E., Papike, J.J., 1968. Bonding in eight ordered clinopyroxenes isostructural with diopside. Contrib. Mineral. Petrol. 20 (1), 81–85.

Czas, J., Stachel, T., Pearson, D.G., Stern, R.A., Read, G.H., 2018. Diamond brecciation and annealing accompanying major metasomatism in eclogite xenoliths from the Sask Craton. Canada. Mineral. Petrol. 112 (S1), 311–323. https://doi.org/10.1007/s00710-018-0590-y.

Dasgupta, R., Hirschmann, M.M., 2010. The deep carbon cycle and melting in Earth's interior. Earth Planet. Sci. Lett. 298 (1–2), 1–13. https://doi.org/10.1016/j.epsl.2010.06.039.

Eom, J., Yoshimura, T., Akizawa, N., Wakaki, S., Ishikawa, T., Takazawa, E., et al., 2022. The magnesium isotopic compositions of the crust and mantle: A study on the Oman ophiolite. Chem. Geol. 606, 120969. https://doi.org/10.1016/j.chemgeo.2022.120969.

Foley, S.F., Fischer, T.P., 2017. An essential role for continental rifts and lithosphere in the deep carbon cycle. Nat. Geosci. 10 (12), 897–902. https://doi.org/10.1038/s41561-017-0002-7.

Garbe-Schönberg, D., Koepke, J., Müller, S., Mock, D., Müller, T., 2022. A reference section through Fast-Spread lower oceanic crust, Wadi Gideah, Samail Ophiolite (Sultanate of Oman): Whole rock geochemistry. J. Geophys. Res. Solid Earth 127 (6), e2021JB022734. https://doi.org/10.1029/2021JB022734.

Gernon, T.M., Barr, R., Fitton, J.G., Hincks, T.K., Keir, D., Longman, J., et al., 2022. Transient mobilization of subcrustal carbon coincident with Palaeocene-Eocene Thermal Maximum. Nat. Geosci. 15 (7), 573–579. https://doi.org/10.1038/s41561-022-00967-6.

Giuliani, A., Drysdale, R.N., Woodhead, J.D., Planavsky, N.J., Phillips, D., Hergt;, J., et al., 2022. Perturbation of the deep-Earth carbon cycle in response to the Cambrian Explosion. Sci. Adv. 8 (9), eabj1325. https://doi.org/10.1126/sciadv.abj1325.

Gorczyk, W., Gonzalez, C.M., 2019. CO_2 degassing and melting of metasomatized mantle lithosphere during rifting—numerical study. Geosci. Front. 10 (4), 1409–1420. https://doi.org/10.1016/j.gsf.2018.11.003.

Gregory, R.T., Taylor, H.P., 1981. An oxygen isotope profile in a section of Cretaceous oceanic crust, Samail Ophiolite, Oman: Evidence for $\delta^{18}O$ buffering of the oceans by deep (> 5 km) seawater-hydrothermal circulation at mid-ocean ridges. J. Geophys. Res. Solid Earth 86 (B4), 2737–2755. https://doi.org/10.1029/JB086iB04p02737.

Higgins, J.A., Schrag, D.P., 2010. Constraining magnesium cycling in marine sediments using magnesium isotopes. Geochim. Cosmochim. Acta. 74 (17), 5039–5053. https://doi.org/10.1016/j.gca.2010.05.019.

Hills, D.V., Haggerty, S.E., 1989. Petrochemistry of eclogites from the Koidu Kimberlite Complex, Sierra Leone. Contrib. Mineral. Petrol. 103, 397–422. https://doi.org/10.1007/BF01041749.

Hippler, D., Buhl, D., Witbaard, R., Richter, D.K., Immenhauser, A., 2009. Towards a better understanding of magnesium isotope ratios from marine skeletal carbonates. Geochim. Cosmochim. Acta. 73 (20), 6134–6146. https://doi.org/10.1016/j.gca.2009.07.031.

Huang, F., Zhang, Z.F., Lundstrom, C.C., Zhi, X.C., 2011. Iron and magnesium isotopic compositions of peridotite xenoliths from Eastern China. Geochim. Cosmochim. Acta. 75 (12), 3318–3334. https://doi.org/10.1016/j.gca.2011.03.036.

Huang, F., Chen, L., Wu, Z., Wang, W., 2013. First-principles calculations of equilibrium Mg isotope fractionations between garnet, clinopyroxene, orthopyroxene, and olivine: Implications for Mg isotope thermometry. Earth Planet. Sci. Lett. 367, 61–70.

Huang, J.X., Li, P., Griffin, W.L., Xia, Q.K., Greau, Y., Pearson, N.J., O'Reilly, S.Y., 2014. Water contents of Roberts Victor xenolithic eclogites: Primary and metasomatic controls. Contrib. Mineral. Petrol. 168 (6), 1092. https://doi.org/10.1007/s00410-014-1092-5.

Huang, J., Huang, J.X., Griffin, W.L., Huang, F., 2022. Zn-, Mg- and O-isotope evidence for the origin of mantle eclogites from Roberts Victor kimberlite (Kaapvaal Craton, South Africa). Geology 50 (5), 593–597. https://doi.org/10.1130/G49780.1.

Hu, Y., Teng, F.-Z., Ionov, D.A., 2020. Magnesium isotopic composition of metasomatized upper sub-arc mantle and its implications to Mg cycling in subduction zones. Geochim. Cosmochim. Acta. 278, 219–234. https://doi.org/10.1016/j.gca.2019.09.030.

Jacob, D.E., 2004. Nature and origin of eclogite xenoliths from kimberlite. Lithos 77 (1–4), 295–316.

Kitajima, K., Strickland, A., Spicuzza, M.J., Tenner, T.J., Valley, J.W., 2016. Improved matrix correction of $\delta^{18}O$ analysis by SIMS for pyralspite and Cr-pyrope garnets. Goldschmidt Abstracts 1542, 2016.

Korolev, N.M., Melnik, A.E., Li, X.H., Skublov, S.G., 2018. The oxygen isotope composition of mantle eclogites as a proxy of their origin and evolution. Earth-Sci. Rev. 185, 288–300. https://doi.org/10.1016/j.earscirev.2018.06.007.

Li, L., Bebout, G.E., Idleman, B.D., 2007. Nitrogen concentration and $d^{15}N$ of altered oceanic crust obtained on ODP legs 129 and 185: insights into alteration-related nitrogen enrichment and the nitrogen subduction budget. Geochim. Cosmochim. Acta 71 (9), 2344–2360. https://doi.org/10.1016/j.gca.2007.02.001.

Li, W.Y., Teng, F.Z., Halama, R., Keller, J., Klaudius, J., 2016. Magnesium isotope fractionation during carbonatite magmatism at Oldoinyo Lengai. Tanzania. Earth Planet. Sci. Lett. 444, 26–33. https://doi.org/10.1016/j.epsl.2016.03.034.
Li, S.G., Yang, W., Ke, S., Meng, X., Tian, H., Xu, L.J., et al., 2017. Deep carbon cycles constrained by a large-scale mantle Mg isotope anomaly in eastern China. Natl. Sci. Rev. 4 (1), 111–120. https://doi.org/10.1093/nsr/nww070.
Ling, M.X., Sedaghatpour, F., Teng, F.Z., Hays, P.D., Strauss, J., Sun, W.D., 2011. Homogeneous magnesium isotopic composition of seawater: an excellent geostandard for Mg isotope analysis. Rapid Commun. Mass Spectrom. 25 (19), 2828–2836. https://doi.org/10.1002/rcm.5172.
Liu, D.L., Sun, X.R., Li, Z.S., Tang, A.N., Tan, Y., Liu, B., 2006. Analysis of Carbon and Oxygen isotope on the Ordovician Dolostones in the Ordos Basin. Petroleum Geology and Experiment. 28 (2), 155–161.
Liu, Y.S., Hu, Z.C., Gao, S., Gunther, D., Xu, J., Gao, C.G., Chen, H.H., 2008. In situ analysis of major and trace elements of anhydrous minerals by LA-ICP-MS without applying an internal standard. Chem. Geol. 257 (1–2), 34–43. https://doi.org/10.1016/j.chemgeo.2008.08.004.
Mallik, A., Dasgupta, R., 2013. Reactive infiltration of MORB-eclogite-derived carbonated silicate melt into fertile peridotite at 3 GPa and genesis of alkalic magmas. J. Petrol. 54 (11), 2267–2300. https://doi.org/10.1093/petrology/egt047.
Mattey, D., Lowry, D., Macpherson, C., 1994. Oxygen isotope composition of mantle peridotite. Earth Planet. Sci. Lett. 128 (3–4), 231–241. https://doi.org/10.1016/0012-821X (94) 90147-3.
McDonough, W.F., Sun, S.S., 1995. The composition of the Earth. Chem. Geol. 120 (3–4), 223–253. https://doi.org/10.1016/0009- 2541(94)00140-4.
Meister, P., Gutjahr, M., Frank, M., Bernasconi, S.M., Vasconcelos, C., Mckenzie, J.A., 2011. Dolomite formation within the methanogenic zone induced by tectonically driven fluids in the Peru accretionary prism. Geology 39 (6), 563–566. https://doi.org/10.1130/G31810.1.
Muller, R.D., Mather, B., Dutkiewicz, A., Keller, T., Merdith, A., Gonzalez, C.M., et al., 2022. Evolution of Earth's tectonic carbon conveyor belt. Nature 605 (7911), 629–639. https://doi.org/10.1038/s41586-022-04420-x.
O'Reilly, S.Y., Griffin, W., 2013. Moho vs crust-mantle boundary: Evolution of an idea. Tectonophysics 609, 535–546. https://doi.org/10.1016/j.tecto.2012.12.031.
Page, F.Z., Kita, N.T., Valley, J.W., 2010. Ion microprobe analysis of oxygen isotopes in garnets of complex chemistry. Chem. Geol. 270 (1–4), 9–19. https://doi.org/10.1016/j.chemgeo.2009.11.00.
Petrash, D.A., Bialik, O.M., Bontognali, T.R.R., Vasconcelos, C., Roberts, J.A., McKenzie, J.A., Konhauser, K.O., 2017. Microbially catalyzed dolomite formation: From near-surface to burial. Earth-Sci. Rev. 171, 558–582. https://doi.org/10.1016/j.earscirev.2017.06.015.
Pogge von Strandmann, P.A.E., 2008. Precise magnesium isotope measurements in core top planktic and benthic foraminifera. Geochem., Geophys., Geosyst. 9 (12), 1–13. https://doi.org/10.1029/2008GC002209.
Qiao, X.Y., Xiong, J.W., Chen, Y.X., De, H.J.C.M., Huang, F., Zhao, Z.F., Chen, K., 2025. Magnesium and boron isotope evidence for the generation of arc magma through serpentinite-mélange melting. Natl. Sci. Rev. 12, nwae363.
Qi, Q., Taylor, L.A., Zhou, X., 1994. Geochemistry and petrogenesis of three series of Cenozoic basalts from southeastern China. Int. Geol. Rev. 36 (5), 435–451. https://doi.org/10.1080/00206819409465470.
Radu, I.B., Harris, C., Moine, B.N., Costin, G., 2019. Subduction relics in the subcontinental lithospheric mantle evidence from variation in the $d^{18}O$ value of eclogite xenoliths from the Kaapvaal craton. Contrib. Mineral. Petrol. 174, 19. https://doi.org/10.1007/s00410-019-1552-z.
Riches, A.J.V., Ickert, R.B., Pearson, D.G., Stern, R.A., Jackson, S.E., Ishikawa, A., et al., 2016. In situ oxygen-isotope, major-, and trace-element constraints on the metasomatic modification and crustal origin of a diamondiferous eclogite from Roberts Victor. Kaapvaal Craton. Geochim. Cosmochim. Acta 174, 345–359. https://doi.org/10.1016/j.gca.2015.11.028.
Richter, F.M., Dauphas, N., Teng, F.Z., 2009. Non-traditional fractionation of non-traditional isotopes: Evaporation, chemical diffusion and Soret diffusion. Chem. Geol. 258 (1–2), 92–103. https://doi.org/10.1016/j.chemgeo.2008.06.011.
Smart, K.A., Heaman, L.M., Chacko, T., Simonetti, A., Kopylova, M., Mah, D., Daniels, D., 2009. The origin of high-MgO diamond eclogites from the Jericho kimberlite. Canada. Earth Planet. Sci. Lett. 284 (3–4), 527–537. https://doi.org/10.1016/j.epsl.2009.05.020.
Sobolev, S.V., Sobolev, A.V., Kuzmin, D.V., Krivolutskaya, N.A., Petrunin, A.G., Arndt, N. T., et al., 2011. Linking mantle plumes, large igneous provinces and environmental catastrophes. Nature 477 (7364), 312–316. https://doi.org/10.1038/nature10385.
Spengler, D., Alifirova, T.A., 2019. Formation of Siberian cratonic mantle websterites from high-Mg magmas. Lithos 326–327, 384–396. https://doi.org/10.1016/j.lithos.2018.12.02.
Stachel, T., Luth, R.W., 2015. Diamond formation-where, when and how? Lithos 220–223 (suppl.2), 200–220. https://doi.org/10.1016/j.lithos.2015.01.028.
Stachel, T., Aulbach, S., Harris, J.W., 2022. Mineral inclusions in lithospheric diamonds. Rev. Mineral. Geochem. 88 (1), 307–391. https://doi.org/10.2138/rmg.2022.88.06.
Stagno, V., Ojwang, D.O., McCammon, C.A., Frost, D.J., 2013. The oxidation state of the mantle and the extraction of carbon from Earth's interior. Nature 493 (7430), 84–88. https://doi.org/10.1038/nature11679.
Sun, J., Rudnick, R.L., Kostrovitsky, S., Kalashnikova, T., Kitajima, K., Li, R.P., Shu, Q., 2020. The origin of low-MgO eclogite xenoliths from Obnazhennaya kimberlite. Siberian craton. Contrib. Mineral. Petrol. 175, 25. https://doi.org/10.1007/s00410-020-1655-6.
Sun, J., Mitchell, N.R., Kostrovitsky, S., Apen, F., 2022. Siberia's largest pulse of kimberlite-s: U-Pb geochronology of perovskite and rutile from the Obnazhennaya kimberlite and its xenoliths. Siberia craton. Int. Geol. Rev. 64 (12), 1743–1754. https://doi.org/10.1080/00206814.2021.19583844.
Sun, J., Tappe, S., Kostrovitsky, S., Kalashnikova, T., Zhou, S.H., 2025. Timing of subduction along the northern margin of the Siberian craton: Lu-Hf and Sm-Nd isochrons for kimberlite-borne mantle eclogite xenoliths. Lithos 508–509, 108062. https://doi.org/10.1016/j.lithos.2025.108062.
Tappe, S., Smart, K.A., Pearson, D.G., Steenfelt, A., Simonetti, A., 2011. Craton formation in Late Archean subduction zones revealed by first Greenland eclogites. Geology 39 (12), 1103–1106. https://doi.org/10.1130/G32348.1.
Taylor, L.A., Snyder, G.A., Keller, R., Remley, D.A., Anand, M., Wiesli, R., et al., 2003. Petrogenesis of group A eclogites and websterites: evidence from the Obnazhennaya kimberlite. Yakutia. Contrib. Mineral. Petrol. 145, 424–443. https://doi.org/10.1007/s00410-003-0465-y.
Teng, F.Z., 2017. Magnesium isotope geochemistry. Rev. Mineral. Geochem. 82 (1), 219–287. https://doi.org/10.2138/rmg.2017.82.7.
Teng, F.Z., Li, W.Y., Ke, S., Marty, B., Dauphas, N., Huang, S.C., et al., 2010. Magnesium isotopic composition of the Earth and chondrites. Geochim. Cosmochim. Acta 74 (14), 4150–4166. https://doi.org/10.1016/j.gca.2010.04.019.
Tipper, E.T., Galy, A., Bickle, M.J., 2006. Riverine evidence for a fractionated reservoir of Ca and Mg on the continents: implications for the oceanic Ca cycle. Earth Planet. Sci. Lett. 247 (3–4), 267–279. https://doi.org/10.1016/j.epsl.2006.04.033.
Valley, J.W., Kitchen, N., Kohn, M.J., Niendorf, C.R., Spicuzza, M.J., 1995. UWG-2, a garnet standard for oxygen isotope ratios: Strategies for high precision and accuracy with laser heating. Geochim. Cosmochim. Acta 59 (24), 5223–5231. https://doi.org/10.1016/0016-7037(95)00386-X.
Wang, S.J., Teng, F.Z., Li, S.G., 2014. Tracing carbonate-silicate interaction during subduction using magnesium and oxygen isotopes. Nat. Commun. 5 (1), 5238. https://doi.org/10.1038/ncomms6328.
Wang, S.J., Teng, F.Z., Rudnick, R.L., Li, S.G., 2015. Magnesium isotope evidence for a recycled origin of cratonic eclogites. Geology 43 (12), 1071–1074. https://doi.org/10.1130/G37259.1.
Wang, X.J., Chen, L.H., Hofmann, A.W., Takeshi, H., Hiroshi, K., Zhong, Y., et al., 2018. Recycled ancient ghost carbonate in the pitcairn mantle plume. Proc. Natl. Acad. Sci. 115 (35), 201719570. https://doi.org/10.1073/pnas.1719570115.
Wombacher, F., Eisenhauer, A., Heuser, A., Weyer, S., 2009. Separation of Mg, Ca and Fe from geological reference materials for stable isotope ratio analyses by MC-ICP-MS and Double-Spike TIMS. J. Anal. At. Spectrom. 24 (5), 627–636. https://doi.org/10.1039/b820154d.
Xiao, Y., Teng, F.Z., Zhang, H.F., Yang, W., 2013. Large magnesium isotope fractionation in peridotite xenoliths from eastern North China craton: Product of melt–rock interaction. Geochim. Cosmochim. Acta 115, 241–261. https://doi.org/10.1016/j.gca.2013.04.011.
Xu, J.Y., Giuliani, A., Li, Q.L., Lu, K., Melgarejo, J.C., Griffin, W.L., 2021. Light oxygen isotopes in mantle-derived magmas reflect assimilation of sub-continental lithospheric mantle material. Nat. Commun. 12 (1), 6295. https://doi.org/10.1038/s41467-021-26668-z.
Young, E.D., Galy, A., 2004. The isotope geochemistry and cosmochemistry of magnesium. Rev. Mineral. Geochem. 55 (1), 197–230. https://doi.org/10.2138/gsrmg.55.1.197.
Zhang, X.Y., Chen, L.H., Wang, X.J., Han, Y.T., Hofmann, A.W., Komiya, T., et al., 2022. Zinc isotopic evidence for recycled carbonate in the deep mantle. Nat. Commun. 13 (1), 6085. https://doi.org/10.1038/s41467-02203378906.
Zhao, X.M., Zhang, Z.F., Huang, S.C., Liu, Y.F., Li, X., Zhang, H., F., 2017. Coupled extremely light Ca and Fe isotopes in peridotites. Geochim. Cosmochim. Acta 208, 368–380. https://doi.org/10.1016/j.gca.2017.03.024.